The Astrophysical Journal Letters, 967:L37 (9pp), 2024 June 1 https://doi.org/10.3847/2041-8213/ad4648

Lensed Type Ia Supernova "Encore" at $z = 2$: The First Instance of Two Multiply Imaged Supernovae in the Same Host Galaxy

J. D. R. Pierel[1,39], A. B. Newman[2], S. Dhawan[3], M. Gu[4], B. A. Joshi[5], T. Li[6], S. Schuldt[7,8], L. G. Strolger[1], S. H. Suyu[9,10,11], G. B. Caminha[9,10], S. H. Cohen[12], J. M. Diego[13], J. C. J. DSilva[14,15], S. Ertl[9,10], B. L. Frye[16], G. Granata[7,8,17], C. Grillo[7,8], A. M. Koekemoer[1], J. Li[14], A. Robotham[14], J. Summers[12], T. Treu[18], R. A. Windhorst[12], A. Zitrin[19], S. Agarwal[20], A. Agrawal[21], N. Arendse[22], S. Belli[23], C. Burns[2], R. Cañameras[9,10], S. Chakrabarti[24], W. Chen[25], T. E. Collett[6], D. A. Coulter[1], R. S. Ellis[26], M. Engesser[1], N. Foo[12], O. D. Fox[1], C. Gall[27], N. Garuda[16], S. Gezari[1], S. Gomez[1], K. Glazebrook[28], J. Hjorth[27], X. Huang[29,30], S. W. Jha[31], P. S. Kamieneski[12], P. Kelly[32], C. Larison[31], L. A. Moustakas[33], M. Pascale[20], I. Pérez-Fournon[34,35], T. Petrushevska[36], F. Poidevin[34,35], A. Rest[1,5], M. Shahbandeh[1], A. J. Shajib[30,37,39], M. Siebert[1], C. Storfer[38], M. Talbot[33], Q. Wang[5], T. Wevers[1], and Y. Zenati[1,5,40]

[1] Space Telescope Science Institute, Baltimore, MD 21218, USA; jpierel@stsci.edu
[2] Observatories of the Carnegie Institution for Science, 813 Santa Barbara Street, Pasadena, CA 91101, USA
[3] Institute of Astronomy and Kavli Institute for Cosmology, University of Cambridge, Madingley Road, Cambridge CB3 0HA, UK
[4] Department of Physics, The University of Hong Kong, Pok Fu Lam, Hong Kong
[5] Physics and Astronomy Department, Johns Hopkins University, Baltimore, MD 21218, USA
[6] Institute of Cosmology and Gravitation, University of Portsmouth, Burnaby Road, Portsmouth, PO1 3FX, UK
[7] Dipartimento di Fisica, Università degli Studi di Milano, via Celoria 16, I-20133 Milano, Italy
[8] INAF—IASF Milano, via A. Corti 12, I-20133 Milano, Italy
[9] Technical University of Munich, TUM School of Natural Sciences, Physics Department, James-Franck-Str. 1, 85748 Garching, Germany
[10] Max-Planck-Institut für Astrophysik, Karl-Schwarzschild-Str. 1, D-85748 Garching, Germany
[11] Institute of Astronomy and Astrophysics, Academia Sinica, 11F of ASMAB, No. 1, Section 4, Roosevelt Road, Taipei 10617, Taiwan
[12] School of Earth and Space Exploration, Arizona State University, Tempe, AZ 85287-1404, USA
[13] Instituto de Fisica de Cantabria (CSIC-C). Avda. Los Castros s/n. 39005 Santander, Spain
[14] International Centre for Radio Astronomy Research (ICRAR) and the International Space Centre (ISC), The University of Western Australia, M468, 35 Stirling Highway, Crawley, WA 6009, Australia
[15] ARC Centre of Excellence for All Sky Astrophysics in 3 Dimensions (ASTRO 3D), Australia
[16] Department of Astronomy/Steward Observatory, University of Arizona, 933 N. Cherry Avenue, Tucson, AZ 85721, USA
[17] Dipartimento di Fisica e Scienze della Terra, Università degli Studi di Ferrara, via Saragat 1, I-44122 Ferrara, Italy
[18] Physics and Astronomy Department, University of California, Los Angeles, CA 90095, USA
[19] Department of Physics, Ben-Gurion University of the Negev, P.O. Box 653, Beer-Sheva, 84105, Israel
[20] Department of Astronomy, University of California, 501 Campbell Hall #3411, Berkeley, CA 94720, USA
[21] Department of Astronomy, University of Illinois, Urbana, IL 61801, USA
[22] Oskar Klein Centre, Department of Physics, Stockholm University, SE-106 91 Stockholm, Sweden
[23] Dipartimento di Fisica e Astronomia, Universitá di Bologna, via Piero Gobetti 93/2, 40129 Bologna, Italy
[24] Department of Physics and Astronomy, University of Alabama, 301 Sparkman Drive, Huntsville, AL 35899, USA
[25] Department of Physics, Oklahoma State University, 145 Physical Sciences Building, Stillwater, OK 74078, USA
[26] University College London, Gower Street, London WC1E 6BT, UK
[27] DARK, Niels Bohr Institute, University of Copenhagen, Jagtvej 155, 2200 Copenhagen, Denmark
[28] Centre for Astrophysics and Supercomputing, Swinburne University of Technology, P.O. Box 218, Hawthorn, VIC 3122, Australia
[29] Department of Physics & Astronomy, University of San Francisco, San Francisco, CA 94117-1080, USA
[30] Kavli Institute for Cosmological Physics, University of Chicago, Chicago, IL 60637, USA
[31] Department of Physics and Astronomy, Rutgers University, 136 Frelinghuysen Road, Piscataway, NJ 08854, USA
[32] Minnesota Institute for Astrophysics, 116 Church Street SE, Minneapolis, MN 55455, USA
[33] Jet Propulsion Laboratory, California Institute of Technology, 4800 Oak Grove Drive, Pasadena, CA 91109, USA
[34] Instituto de Astrofísica de Canarias, Vía Láctea, 38205 La Laguna, Tenerife, Spain
[35] Universidad de La Laguna, Departamento de Astrofísica, 38206 La Laguna, Tenerife, Spain
[36] Center for Astrophysics and Cosmology, University of Nova Gorica, Vipavska 11c, 5270 Ajdovščina, Slovenia
[37] Department of Astronomy & Astrophysics, The University of Chicago, Chicago, IL 60637, USA
[38] Institute for Astronomy, University of Hawaii, Honolulu, HI 96822-1897, USA
Received 2024 April 2; revised 2024 April 26; accepted 2024 May 2; published 2024 May 29

Abstract

A bright ($m_{\mathrm{F150W,AB}} = 24$ mag), $z = 1.95$ supernova (SN) candidate was discovered in JWST/NIRCam imaging acquired on 2023 November 17. The SN is quintuply imaged as a result of strong gravitational lensing by a foreground galaxy cluster, detected in three locations, and remarkably is the second lensed SN found in the same host galaxy. The previous lensed SN was called "Requiem," and therefore the new SN is named "Encore." This

[39] NASA Einstein Fellow.
[40] ISEF International Fellowship.

makes the MACS J0138.0−2155 cluster the first known system to produce more than one multiply imaged SN. Moreover, both SN Requiem and SN Encore are Type Ia SNe (SNe Ia), making this the most distant case of a galaxy hosting two SNe Ia. Using parametric host fitting, we determine the probability of detecting two SNe Ia in this host galaxy over a ∼10 yr window to be ≈3%. These observations have the potential to yield a Hubble constant (H_0) measurement with ∼10% precision, only the third lensed SN capable of such a result, using the three visible images of the SN. Both SN Requiem and SN Encore have a fourth image that is expected to appear within a few years of ∼2030, providing an unprecedented baseline for time-delay cosmography.

Unified Astronomy Thesaurus concepts: Gravitational lensing (670); Cosmology (343); Type Ia supernovae (1728); Supernovae (1668); Galaxy clusters (584)

1. Introduction

Strong gravitational lensing can cause multiple images of a background source to appear, as light propagating along different paths are focused by the gravity of a foreground galaxy or galaxy cluster (called the "lens"; e.g., Narayan & Bartelmann 1997). Such a phenomenon requires chance alignment between the observer, the background source, and the lens. If the multiply imaged source has variable brightness, then depending on the relative geometrical and gravitational potential differences of each path, the source images will typically appear delayed by hours to weeks (for galaxy-scale lenses, $M \lesssim 10^{12}\ M_{\odot}$) or months to years (for cluster-scale lenses, $M \gtrsim 10^{13}\ M_{\odot}$; e.g., Oguri 2019).

Precise measurements of this "time delay" yield a direct distance measurement to the lens system that constrains the Hubble constant (H_0) in a single step (e.g., Refsdal 1964; Paraficz & Hjorth 2009; Linder 2011; Treu & Marshall 2016; Grillo et al. 2018, 2020, 2024; Birrer et al. 2022b; Treu et al. 2022; Kelly et al. 2023a; Suyu et al. 2024). While this has been accomplished with quasars (e.g., Kundić et al. 1997; Schechter et al. 1997; Burud et al. 2002; Hjorth et al. 2002; Vuissoz et al. 2008; Suyu et al. 2010; Tewes et al. 2013; Bonvin et al. 2017, 2018, 2019; Birrer et al. 2019, 2020; Chen et al. 2019; Shajib et al. 2020, 2023; Wong et al. 2020), there is much discussion about the advantages of using supernovae (SNe) instead to leverage a variety of valuable characteristics such as predictable evolution, simplicity of observations, standardizable brightness (for Type Ia SNe, SNe Ia), and mitigated microlensing effects (e.g., Foxley-Marrable et al. 2018; Goldstein et al. 2018; Pierel & Rodney 2019; Ding et al. 2021; Huber et al. 2021; Pierel et al. 2021, 2024; Birrer et al. 2022a; Chen et al. 2024; Pascale et al. 2024). The sample of strongly lensed SNe has grown over the last decade to include two galaxy-scale systems (Goobar et al. 2017, 2023; Pierel et al. 2023) and five cluster-scale systems (Kelly et al. 2015; Rodney et al. 2021; Chen et al. 2022; Kelly et al. 2022; Frye et al. 2024) though only SN Refsdal (Kelly et al. 2023a, 2023b) and SN H0pe (Chen et al. 2024; Frye et al. 2024; Pascale et al. 2024; Pierel et al. 2024) have had sufficiently long time delays and well-sampled light curves for H_0 constraints with relatively small uncertainty. SN Refsdal yielded a ∼6% measurement of H_0 in flat ΛCDM cosmology ($64.8^{+4.4}_{-4.3}$ or $66.6^{+4.1}_{-3.3}$ km s^{-1} Mpc^{-1}, depending on lens model weights; Kelly et al. 2023a) and also $65.1^{+3.5}_{-3.4}$ km s^{-1} Mpc^{-1} in more general background cosmological models (Grillo et al. 2024). SN H0pe is of particular interest as the first lensed SN Ia to provide an H_0 result competitive with local measurements, resulting in $75.4^{+8.1}_{-5.5}$ km s^{-1} Mpc^{-1} (Pascale et al. 2024).

SNe Ia are of particular value when strongly lensed, as their standardizable absolute brightness can provide additional leverage for lens modeling by limiting the uncertainty caused by the mass-sheet degeneracy (Falco et al. 1985; Kolatt & Bartelmann 1998; Holz 2001; Oguri & Kawano 2003; Nordin et al. 2014; Patel et al. 2014; Rodney et al. 2015; Xu et al. 2016; Foxley-Marrable et al. 2018; Birrer et al. 2022a) though only in cases where millilensing and microlensing are not extreme (see Goobar et al. 2017; Yahalomi et al. 2017; Foxley-Marrable et al. 2018; Dhawan et al. 2020). Additionally, SNe Ia have well-understood models of light-curve evolution (Hsiao et al. 2007; Guy et al. 2010; Saunders et al. 2018; Leget et al. 2020; Kenworthy et al. 2021; Mandel et al. 2022; Pierel et al. 2022) that enable precise time-delay measurements using color curves, which removes the effects of macro- and achromatic microlensing (e.g., Pierel & Rodney 2019; Huber et al. 2021; Rodney et al. 2021; Pierel et al. 2023). Both iPTF16geu (Goobar et al. 2017) and SN Zwicky (Goobar et al. 2023; Pierel et al. 2023) were SNe Ia, but each had very short time delays of ∼0.25–1.5 days that precluded competitive H_0 measurements (Dhawan et al. 2020; Pierel et al. 2023).

SN Requiem (Rodney et al. 2021) was the first cluster-scale *photometrically* classified multiply imaged SN Ia, appearing at $z = 1.95$ in the MRG-M0138 galaxy that is lensed by the MACS J0138.0−2155 cluster (Figure 1). Unfortunately, the SN was found archivally several years after it had faded, precluding an H_0 measurement with the visible images. However, there is a fourth image of SN Requiem expected in ∼2035, an astounding ∼20 yr time delay (Rodney et al. 2021). In a truly remarkable turn of events, a second lensed SN Ia (dubbed SN Encore) has been found by the James Webb Space Telescope (JWST) in the same host galaxy as SN Requiem at $z = 1.95$. The discovery visit was on 2023 November 17 (JWST-GO-2345, PI: Newman), which included JWST NIRCam imaging and NIRSpec integral field unit (IFU) observations. Previous observations of MACS J0138.0−2155 and MRG-M0138 are described in Newman et al. (2018, hereafter N18), and SN Requiem is described in Rodney et al. (2021).

This work presents the discovery and observations of SN Encore and is the start of a series of papers analyzing the system. The outline of this Letter is as follows: Section 2 summarizes the Hubble Space Telescope (HST) and JWST observations taken to follow SN Encore. Section 3 leverages the spectrum from Section 2 to identify SN Encore as an SN Ia, while Section 4 discusses our expectations surrounding the discovery of a second lensed SN Ia in the same host galaxy. We conclude with a discussion of the implications for SN Encore in Section 5.

2. Summary of Observations

SN Encore was discovered by the JWST-GO-2345 team in F150W NIRCam imaging taken 2023 November 17 (MJD 60265) by comparing the data with an archival HST Wide Field Camera 3(WFC3)/infrared (IR) F160W image (2016 July 18,

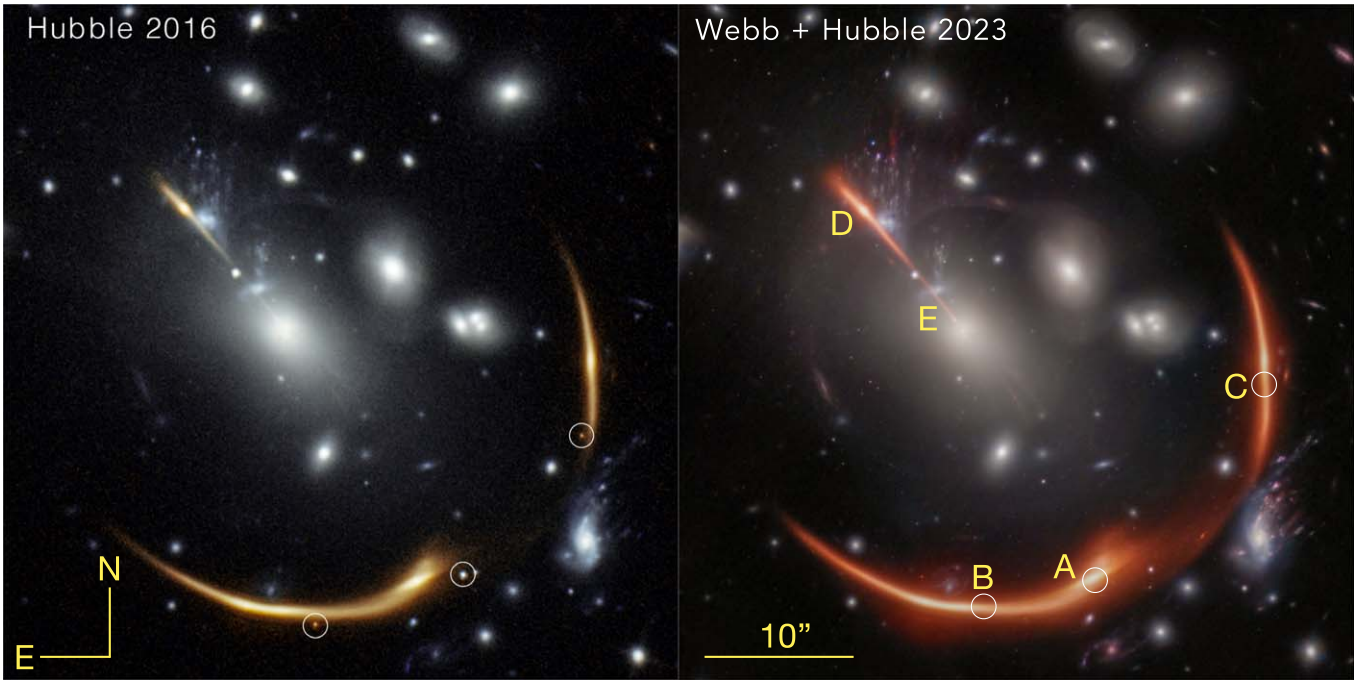

Figure 1. Left: HST WFC3/IR two-color image in the region of MACS J0138.0−2155 from 2016, using F105W (blue) and F160W (orange). SN Requiem is marked in its three visible image positions by white circles, notably absent in 2023. Right: combined JWST/NIRCam and HST/WFC3 color image from programs 6549 and 16264 (Table 1). The filters used are F105W+F115W+F125W (blue), F150W+F160W+F200W (green), and F277W+F356W+F444W (red). The images were drizzled to $0\farcs02$ pix^{-1}, and the image scale and orientation are as shown. The three detected image positions of SN Encore are circled, but it is not visible at this scale, and all five images of the host galaxy are labeled (A–E). For a zoom-in of each of the detected image positions, see Section 2 (Image Credit: STScI, A. Koekemoer, T. Li).

MJD 57587; N18). These two filters are extremely well matched in wavelength and transmission, and the source was very bright ($\lesssim$24 mag AB in both images A and B) in F150W but absent in F160W. However, the separation of SN Encore from its host galaxy MRG-M0138 is only $\sim0\farcs1$, which is roughly the pixel scale of the HST WFC3/IR imaging. We therefore also compared the point-source positions and relative brightnesses to lens model predictions (S. Ertl et al. 2024, in preparation; S. Suyu et al. 2024, in preparation) and confirmed with forced photometry that there was an increase in flux corresponding to the apparent brightness of SN Encore between the F160W and F150W imaging. All tests were in agreement that this was indeed a multiply imaged SN, with (at least) two images of the SN detected (images A and B; see Figure 1). Further efforts to remove host-galaxy light near image C revealed that a third image of SN Encore was also detected. There were two additional images of the host galaxy located in the northeast of the cluster (Figure 1), with the next image of SN Encore expected from our lens modeling to arrive in about a decade (S. Ertl et al. 2024, in preparation). The sharp radial profile of images D and E for MRG-M0138 will provide relatively tight constraints on these long time delays, which will enable a targeted follow-up campaign similar to SN Refsdal (Kelly et al. 2016). N18 reported a spectroscopic redshift for MRG-M0138 of $z = 1.95$, and the host properties alone suggested that SN Encore was likely an SN Ia at $z = 1.95$ (Rodney et al. 2021).

2.1. JWST Data

2.1.1. Imaging

An HST program was triggered soon after the discovery of SN Encore, which is described in Section 2.2. However, JWST was still required for two reasons: (1) the small host separation described above meant that even with difference imaging, it would be very difficult to detect SN Encore in any but the brightest filter (F160W for HST), and (2) based on the discovery epoch, SN Encore was between peak brightness and the second IR maximum for SNe Ia (Hsiao et al. 2007; Krisciunas et al. 2017; Pierel et al. 2022). At $z = 1.95$, HST is only able to cover rest-frame UBV filters, meaning JWST was needed to reach the rest-frame near-IR (NIR) and leverage the second IR maximum for time-delay measurements.

A disruptive JWST director's discretionary time proposal was subsequently approved (JWST-GO-6549, PI: Pierel), which provided three additional epochs of NIRCam imaging in six filters (Table 1; Figure 2). The first NIRCam epoch occurred on 2023 December 5 (MJD 60283), 18 ($\sim$6 rest-frame) days after discovery. The next two epochs took place with a cadence of $\sim$17 observer-frame ($\sim$6 rest-frame) days, on 2023 December 23 (MJD 60301) and 2024 January 8 (MJD 60317). This meant the JWST light curve for each image contains four observations, each separated by $\sim$6 rest-frame days. Although image C of SN Encore is too faint to see clearly by eye in Figure 3, it is $\sim$27 AB mag in F150W and detected at $\sim5\sigma$ with careful subtraction of the host-galaxy light profile in JWST imaging. The full JWST data set therefore effectively produces an SN Ia light curve with 12 epochs and rest-frame UV-NIR wavelength coverage, which is sufficient to accurately measure phases of each image and therefore the relative time delays (e.g., Pierel & Rodney 2019). The summary of observations is given in Table 1.

All the NIRCam data were retrieved from the STScI MAST[41] archive and were processed and calibrated using the

[41] https://mast.stsci.edu

Table 1
Summary of Observations Taken of SN Encore

Program ID	Obs. Type	Telescope	Instrument	MJD	Filter/Grating	Exp. Time (s)
2345	Imaging	JWST	NIRCam	60265	F150W	773
2345	Imaging	JWST	NIRCam	60265	F444W	773
2345	Spectroscopy	JWST	NIRSpec IFU	60266	G235M	7586
2345	Spectroscopy	JWST	NIRSpec IFU	60305	G140M	8170
6549	Imaging	JWST	NIRCam	60283	F115W	1417
6549	Imaging	JWST	NIRCam	60283	F150W	859
6549	Imaging	JWST	NIRCam	60283	F200W	859
6549	Imaging	JWST	NIRCam	60283	F277W	859
6549	Imaging	JWST	NIRCam	60283	F356W	859
6549	Imaging	JWST	NIRCam	60283	F444W	1417
6549	Imaging	JWST	NIRCam	60301	F115W	1589
6549	Imaging	JWST	NIRCam	60301	F150W	1074
6549	Imaging	JWST	NIRCam	60301	F200W	1074
6549	Imaging	JWST	NIRCam	60301	F277W	1074
6549	Imaging	JWST	NIRCam	60301	F356W	1074
6549	Imaging	JWST	NIRCam	60301	F444W	1589
6549	Imaging	JWST	NIRCam	60317	F115W	1589
6549	Imaging	JWST	NIRCam	60317	F150W	1074
6549	Imaging	JWST	NIRCam	60317	F200W	1074
6549	Imaging	JWST	NIRCam	60317	F277W	1074
6549	Imaging	JWST	NIRCam	60317	F356W	1074
6549	Imaging	JWST	NIRCam	60317	F444W	1589
16264	Imaging	HST	WFC3/IR	60294	F105W	6913
16264	Imaging	HST	WFC3/IR	60294	F125W	4609
16264	Imaging	HST	WFC3/IR	60294	F160W	2304
16264	Imaging	HST	WFC3/IR	60339	F105W	9318
16264	Imaging	HST	WFC3/IR	60339	F125W	4609
16264	Imaging	HST	WFC3/IR	60339	F160W	2304

Note. Columns are JWST/HST Program ID, observation type, telescope name, instrument name, Modified Julian Date, filter/grating, and exposure time in seconds.

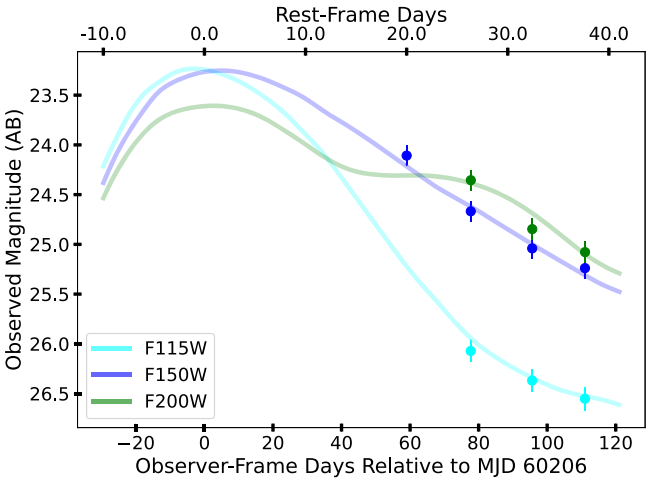

Figure 2. The observed light curve in the JWST/NIRCam short-wavelength filters for image A, the brightest and last to arrive (see Figure 3). The long-wavelength filters (F277W, F356W, and F444W) were observed, but a more in-depth host-galaxy modeling effort (or a template image) will be required to measure accurate photometry.

JWST Pipeline[42] (Bushouse et al. 2022) version 1.12.5, with CRDS reference files defined in 1180.pmap, with additional improvements described here as follows. As part of the initial processing with the Stage 1 portion of the pipeline, additional corrections were applied to remove $1/f$ noise as well as low-level background variations across the detectors, including the removal of wisps and other low-level artifacts, with these techniques all described in more detail in Windhorst et al. (2023). The Stage 2 portion of the pipeline was then run to apply photometric calibration to physical units, using the latest photometric calibrations (Boyer et al. 2022). The images were then all astrometrically aligned directly to the Gaia-DR3[43] reference frame and finally combined into mosaics for each filter with all distortion removed, using the Stage 3 portion of the pipeline, where these mosaics were constructed for each of the individual epochs, as well as full-depth versions combining all the epochs.

2.1.2. Spectroscopy

The JWST-GO-2345 program also included NIRSpec IFU spectroscopy for image A of MRG-M0138 using both the G140M and G235M gratings. There was a failure in the G140M observation, causing it to be scheduled 39 days later on 2023 December 27, but the G235M observation was successful. Here we extract the SN spectrum for the G235M grating, aligned to the G140M spectrum using their overlapping wavelength range, with the G140M spectrum anchored to the F150W NIRCam image to reveal the SN location. The SN spaxels have unique spectral features in the G235M observation, distinct from the galaxy spectra, making it possible to

[42] https://github.com/spacetelescope/jwst

[43] https://www.cosmos.esa.int/web/gaia/dr3

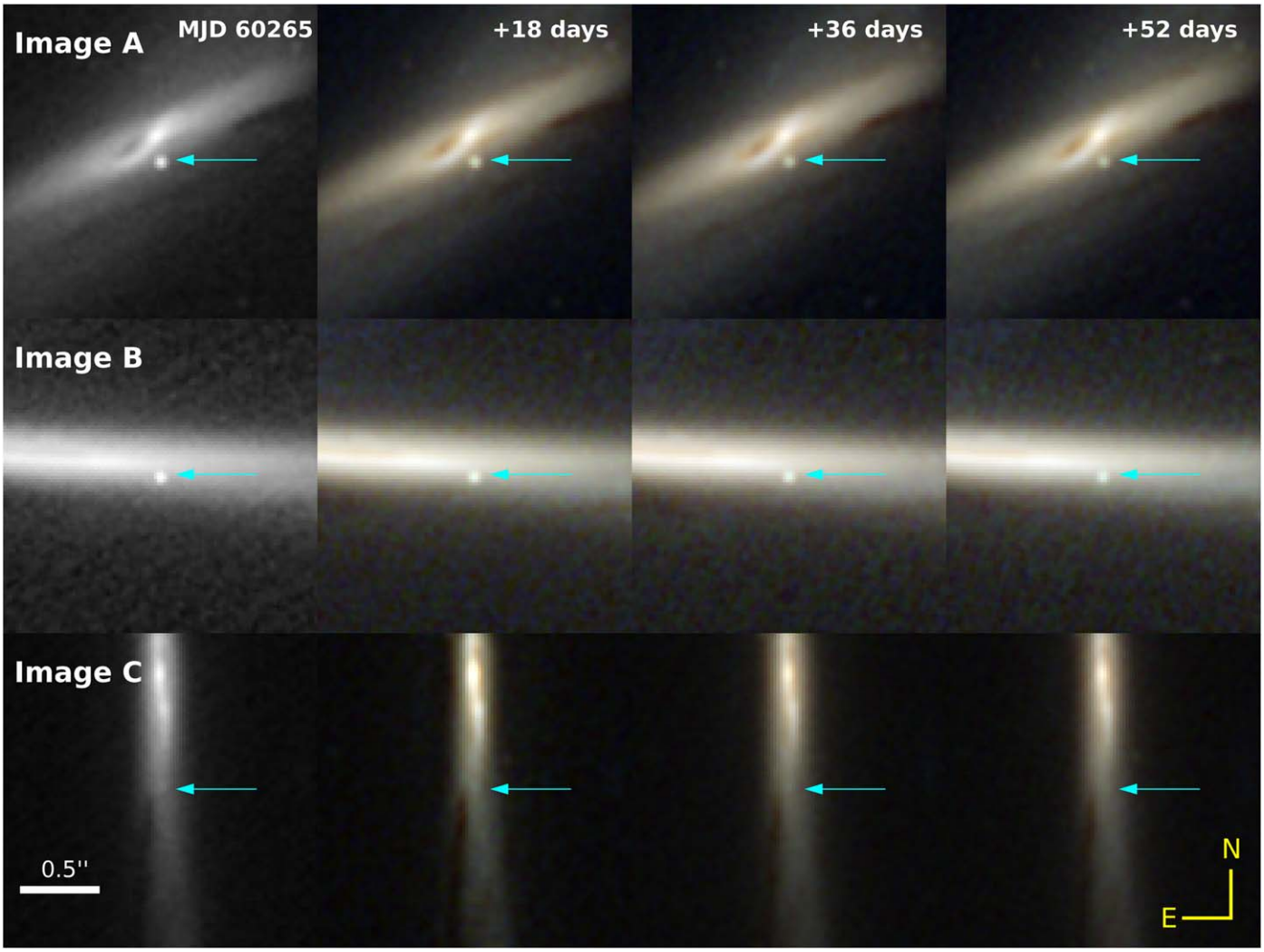

Figure 3. JWST/NIRCam color cutouts with F115W (blue), F150W (green) and F200W (red) centered on image A (top), B (middle), and C (bottom) of SN Encore. Note the discovery program only detected SN Encore in F150W, so the first column is a grayscale image in F150W, while the remainder are three-color images. The images were drizzled to $0\farcs02$ pix^{-1}, with the image scale, orientation, and MJD (relative to discovery) shown. SN Encore is brightest in the discovery epoch and is on the decline in the subsequent epochs, but the evolution is relatively small at this redshift and is therefore difficult to see by eye (see Figure 2). Image C was first to arrive followed by image B, and although image C is not clearly visible by eye, it was detected at $\sim 5\sigma$ (see Section 2.1.1).

disentangle. We establish contour levels for each IFU datacube by calculating the median flux across the entire wavelength range, which allows us to subtract the host-galaxy spectra from the spaxels containing SN flux. Finally, we isolate the SN spectrum by subtracting off the median spectrum of host galaxy from what is observed in the SN spaxels. We leave discussion of the G140M spectrum and in-depth analysis of the G235M spectrum to the upcoming SN spectroscopic analysis (S. Dhawan et al. 2024, in preparation), host-galaxy analysis (D. Newman et al. 2024, in preparation), and investigations into relationships between the host galaxy and SN Ia properties (C. Larison et al. 2024, in preparation). The G235M spectrum is used briefly here to simply confirm the spectroscopic SN type for SN Encore in Section 3 and is shown in Figure 4.

2.2. HST Data

LensWatch[44] is a collaboration with the goal of finding gravitationally lensed SNe, both by monitoring active transient surveys (e.g., Fremling et al. 2020; Jones et al. 2021) and by way of targeted surveys (Craig et al. 2021). The collaboration maintained a Cycle 28 HST program (HST-GO-16264), given long-term (three-cycle) target-of-opportunity (ToO) status. The program included three ToO triggers (two nondisruptive, one disruptive) and was designed to provide high-resolution follow-up imaging for a ground-based lensed SN discovery, which is critical for galaxy-scale multiply imaged SNe due to their small image separations (e.g., Goobar et al. 2017). LensWatch triggered HST-GO program 16264 on 2023 November 20 (MJD 60268, 3 days after discovery) to obtain follow-up imaging of SN Encore, including 14 orbits in three filters spread over two epochs. The trigger was disruptive, but there were small delays related to HST being in safe mode, which led to the first epoch being 26 ($\sim$9 rest-frame) days later on 2023 December 16 (MJD 60294) and the second epoch 45 days after the first on 2024 January 30 (MJD 60339). These observations are separated by 10–22 observer-frame (3–7 rest-frame) days from the JWST observations described in Section 2.1 and were designed to be complementary to JWST. All observations are summarized in Table 1.

[44] https://www.lenswatch.org

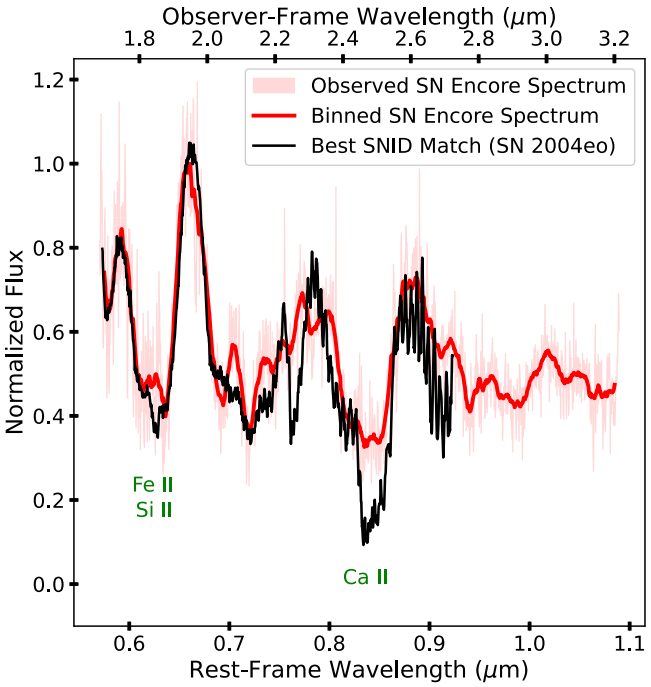

Figure 4. The (normalized) extracted G235M spectrum of SN Encore with 1σ uncertainty (faint red), with the binned spectrum superimposed (thick red line). The best-match spectrum from SNID (SN 2004eo; black line) is shown for comparison, with characteristic SN Ia features labeled in green text, confirming that SN Encore is of Type Ia.

All the HST data were retrieved from the STScI MAST archive, and the calibrated exposures were subsequently processed with additional improvements described here as follows. The default astrometry from the archive was corrected by realigning all the HST exposures to one another, as well as to the JWST images and to Gaia-DR3, using an updated version of the HST "mosaicdrizzle" pipeline first described in Koekemoer et al. (2011), which also removes residual low-level background variations across the detectors. This pipeline was then used to combine all the HST data into mosaics for each filter with all distortion removed, producing mosaics for the separate epochs as well as full-depth versions combining all the epochs.

3. Classifying SN Encore

Lensed SNe Ia offer smaller uncertainties for H_0 than lensed core-collapse SNe (e.g., Goldstein et al. 2018; Pierel & Rodney 2019; Birrer et al. 2022a) and unique leverage on lens modeling systematics (Pascale et al. 2024), making them the most valuable type of lensed SNe. We infer the type of SN Encore using the supernova identification (SNID; Blondin & Tonry 2007) and Next Generation SuperFit (NGSF)[45] packages with the observed G235M spectrum (Table 1; Figure 4). Both packages classify SN Encore as Type Ia with >90% confidence (nine of the top ten best-fit reference spectra are from SNe Ia, and the last is an SN Ia-91T, which is a subclass known to be spectroscopically similar to normal SNe Ia at late times), with the best matches being SN 2004eo (SNID) and SN 2007sr (NGSF). Both of these SNe decline faster than the mean decline rate (SALT3 $x_1 \lesssim 0$), which is in agreement with light-curve fitting for SN Encore ($x_1 \sim -1.3$), but all three SNe exhibit light-curve shapes that are well within traditional cosmology cuts (e.g., $-3 < x_1 < 3$ Scolnic et al. 2018). NGSF also returns an estimate of the host-galaxy contamination in the SN spectrum, which is <1%. Finally, the phase is constrained by the classification codes to 26.5 ± 5.7 rest-frame days, which is in 1.1σ agreement with the results of our light-curve fitting (20.1 ± 3 rest-frame days; Figure 2). Overall, the result of this analysis is therefore that SN Encore is an SN Ia, and moreover is likely a relatively fast-declining SN that should nevertheless be standardizable. A full analysis of both the G235M and G140M spectrum, including a comparison to low-z SN Ia spectra and theoretical models for SN Ia progenitors, will be presented in S. Dhawan et al. (2024, in preparation).

While the most precise time-delay measurements come from lensed SNe observed before peak brightness, a lensed SN Ia observed roughly in the phase of images A and B in multiple filters should still provide a time-delay-measurement uncertainty of ∼5 observer-frame days (Pierel & Rodney 2019). Image C was observed well after peak brightness in the nebular phase of SNe Ia, where the slow and uncertain evolution will likely result in a lower time-delay precision of $\gtrsim$10 observer-frame days (Pierel et al. 2024). Initial expectations from lens models of the MACS J0138.0−2155 cluster and SN Encore photometry suggest the delay between images A and B will be $\gtrsim$1 month, while the delay between images A and C will be ∼1 yr. Assuming a fiducial cluster lens model uncertainty of ∼6% (Grillo et al. 2020; Kelly et al. 2023a), SN Encore should produce an H_0 uncertainty of ∼10%. A detailed lens modeling analysis will be presented by S. Ertl et al. (2024, in preparation) and S. Suyu et al. (2024, in preparation), while measurements of the time delay and H_0 will be presented by J. Pierel et al. (2024, in preparation).

4. Two Lensed SNe Ia from a Single Host Galaxy

While it seems remarkable to find two lensed SNe Ia in the same host galaxy at $z = 1.95$, we briefly explore the probability of such a discovery. A full analysis of the relationship between the local/global properties of MRG-M0138 and both SNe Encore and Requiem will be presented by Larison et al. (2024, in preparation), leveraging the full data set shown in Table 1. Here, we simply provide estimates assuming the results of N18.

N18 describes the specifics of their data acquisition, and here we use their host properties derived from an NIR spectrum from the MOSFIRE spectrograph instrument on the Keck I telescope. N18 have already provided best-fit star formation histories (SFHs) by fitting the MRG-M0138 spectrum with a parametric SFH model. The parametric model they use is of the form SFR $\propto \exp(-t/\tau)$. Table 5 in N18 provides the τ value for the SFH based on two images of MRG-M0138—we adopt an average value of 180 Myr, which is consistent with fits from both images.

There are one of two approaches we investigate here. In the first approach, we assume the SN Ia delay-time distribution (DTD) to be an exponential function from Strolger et al. (2020) and convolve it with our SFHs derived above to obtain an SN Ia rate for MRG-M0138. The SN Ia rate calculation also requires assumptions to be made about the form of the initial mass function (IMF) and the fraction of stars within 3–8 $M_\odot$ that are ultimately successful SN Ia explosions (ϵ). Following Strolger et al. (2020), we assume an IMF with a power-law index of $\alpha \approx -2.3$ (Salpeter 1955; Kroupa 2001) and $\epsilon = 0.06$.

[45] https://github.com/oyaron/NGSF

MRG-M0138 is quiescent and not exceptionally star forming in the observed epoch, at a rate between ≈1.8 and 2.6 (±1.7) $M_\odot$ yr^{-1}, depending on which image is used. Using the method above implies an SN Ia rate of approximately 90 events (1000 yr)$^{-1}$, which is consistent with the average rate of SNe Ia per galaxy, regardless of mass, from Li et al. (2011). Assuming effectively a 10 yr monitoring of the host, i.e., in which no detectable SN Ia event was missed in the last 10 yr (3.39 yr in the rest frame of the host), it would be reasonable to expect the probability of having one SN Ia in that time frame to be low, but not zero, with Pois($k = 1$) = 0.23. Similarly, the probability of finding two such events is also low, with Pois($k = 2$) = 0.03. It is interesting to note that assuming a power-law DTD (e.g., Maoz et al. 2012; Freundlich & Maoz 2021) would make the rate at the observed epoch even lower, 5.3 events (1000 yr)$^{-1}$, and the likelihood of observing two supernovae in MRG-M0138 in 10 yr, Pois($k = 2$) = 0.0001.

However, another approach could be to estimate the expected yield from the mass-weighted rates as is done in Smith et al. (2020) and Scolnic et al. (2020). This has the convenience of estimating the rate from the galaxy's current properties but loses the detailed analysis provided by the Strolger et al. (2020) approach. Li et al. (2011) show an average mass-weighted SN Ia rate per galaxy of 0.54 ± 0.12 events per century per 10^{10} $M_\odot$. N18 determine $\log M_*/M_\odot = 11.7 \pm 0.2$ (for both images of the host), resulting in an expected rest-frame yield of about 260 (1000 yr)$^{-1}$, or 0.88 events, in the 10 yr observation window. The probability of having one SN Ia in that time frame would therefore be a bit higher, with Pois($k = 1$) = 0.37, and the probability of finding two such events seemingly more feasible, at ≈16%. Both approaches are broadly consistent with the rate of discovery of SN Ia siblings from Kelsey (2024) and Scolnic et al. (2020).

5. Discussion

Here we presented the discovery and observations of SN Encore, an SN lensed by the MACS J0138.0−2155 cluster and hosted by the galaxy MRG-M0138 at $z = 1.95$. We spectroscopically confirm that SN Encore is of Type Ia, making it just the second lensed SN Ia and third overall lensed SN useful for measuring H_0 with $\lesssim$10% uncertainty. Remarkably, SN Encore is the second lensed SN Ia hosted by MRG-M0138 in the last ∼7 yr, making it the first known case of two lensed SNe from the same host galaxy. While the appearance of two SNe Ia in the same multiply imaged galaxy is remarkable, MRG-M0138 was targeted because it is by far the brightest and most massive ($M_* = 5 \times 10^{11}$ $M_\odot$) among the rare class of magnified quiescent galaxies at $z \gtrsim 2$ (Toft et al. 2017; Akhshik et al. 2023). MRG-M0138's extreme stellar mass, old stellar population, and lack of strong dust attenuation lead to a low but nonnegligible derived probability of $\lesssim$3% for detecting two SNe Ia in the last ∼decade. SN Requiem and SN Encore will both reappear in the next ∼5–10 yr, providing an exceedingly rare opportunity to monitor MACS J0138.0−2156 for two SNe Ia with known reappearance location and time. The resulting baseline will be unprecedented for time-delay cosmography and can provide unique insights into SN Ia physics at $z = 1.95$.

While SN Encore will not break the H_0 tension (e.g., Riess et al. 2022) on its own, it still plays a critical role as the third lensed SN (and second lensed SN Ia) to provide a precise measurement of H_0. With a sample of three, the combined H_0 uncertainty could plausibly be ∼5%, and we will start to have a clearer picture of the relative agreement across lensed SN measurements of H_0. Upcoming surveys such as the Vera C. Rubin Observatory Legacy Survey of Space and Time (Ivezic et al. 2019; Arendse et al. 2023) and the Nancy Grace Roman Space Telescope High Latitude Time Domain Survey (Pierel et al. 2021; Rose et al. 2021) are expected to deliver dozens of useful galaxy- and cluster-scale multiply imaged SNe, and although more complicated, clusters provide longer time delays, wider image separations, and extra lens modeling constraints on the mass-sheet degeneracy (Falco et al. 1985; Grillo et al. 2020, 2024; Pascale et al. 2024). As a result, cluster-lensed SNe are likely to continue as an extremely valuable subset of the future cosmological sample.

Acknowledgments

This Letter is based in part on observations with the NASA/ESA Hubble Space Telescope and James Webb Space Telescope obtained from the Mikulski Archive for Space Telescopes at STScI. We thank the DDT and JWST/HST scheduling teams at STScI for extraordinary effort in getting the DDT observations used here scheduled quickly. The specific observations analyzed can be accessed via doi:10.17909/snj9-an10; support was provided to J.D.R.P. and M.E. through program HST-GO-16264. J.D.R.P. is supported by NASA through a Einstein Fellowship grant No. HF2-51541.001 and A.J.S. by HF2-51492 awarded by the Space Telescope Science Institute (STScI), which is operated by the Association of Universities for Research in Astronomy, Inc., for NASA, under contract NAS5-26555. R.A.W. acknowledges support from NASA JWST Interdisciplinary Scientist grants NAG5-12460, NNX14AN10G and 80NSSC18K0200 from GSFC. S.H.S. thanks the Max Planck Society for support through the Max Planck Fellowship. This project has received funding from the European Research Council (ERC) under the European Union's Horizon 2020 research and innovation program (LENSNOVA: grant agreement No. 771776). This research is supported in part by the Excellence Cluster ORIGINS which is funded by the Deutsche Forschungsgemeinschaft (DFG, German Research Foundation) under Germany's Excellence Strategy—EXC-2094—390783311. X.H. acknowledges the University of San Francisco Faculty Development Fund. S.D. acknowledges support from the Marie Curie Individual Fellowship under grant ID 890695 and a Junior Research Fellowship at Lucy Cavendish College. C.G. and G.G. acknowledge support through grant PRIN-MIUR 2020SKSTHZ. F.P. acknowledges support from the Spanish Ministerio de Ciencia, Innovación y Universidades (MICINN) under grant Nos. PID2019-110614GB-C21 and PID2022-141915NB-C21. Support for program GO-2345 was provided by NASA through a grant from the Space Telescope Science Institute, which is operated by the Association of Universities for Research in Astronomy, Inc., under NASA contract NAS 5-03127. K.G. acknowledges support from Australian Research Council Laureate Fellowship FL180100060. This work was supported by research grants (VIL16599, VIL54489) from VILLUM FONDEN. R.A.W. acknowledges support from NASA JWST Interdisciplinary Scientist grants NAG5-12460, NNX14AN10G and 80NSSC18K0200 from GSFC. Support for program JWST GO-04446 was provided by NASA through a grant from the Space Telescope Science Institute, which is operated by the Association of Universities for Research in Astronomy, Inc., under NASA contract NAS 5-26555. S.B. is supported by ERC

StG 101076080. S.S. has received funding from the European Union's Horizon 2022 research and innovation program under the Marie Skłodowska-Curie grant agreement No. 101105167—FASTIDIoUS. C.G. is supported by a VILLUM FONDEN Young Investigator Grant (project number 25501). P.L.K. acknowledges support from NSF AAG-2308051. C.L. acknowledges support from the National Science Foundation Graduate Research Fellowship under grant No. DGE-2233066. R.A.W., S. H.C., and R.A.J. acknowledge support from NASA JWST Interdisciplinary Scientist grants NAG5-12460, NNX14AN10G, and 80NSSC18K0200 from GSFC. This work has received funding from the European Research Council (ERC) under the European Union's Horizon 2020 research and innovation program (LensEra: grant agreement No. 945536). T.C. is funded by the Royal Society through a University Research Fellowship. Part of this research was carried out at the Jet Propulsion Laboratory, California Institute of Technology, under a contract with the National Aeronautics and Space Administration (80NM0018D0004). A.Z. acknowledges support by grant No. 2020750 from the United States-Israel Binational Science Foundation (BSF) and grant No. 2109066 from the United States National Science Foundation (NSF); by the Ministry of Science & Technology, Israel; and by the Israel Science Foundation grant No. 864/23.

ORCID iDs

J. D. R. Pierel https://orcid.org/0000-0002-2361-7201
A. B. Newman https://orcid.org/0000-0001-7769-8660
S. Dhawan https://orcid.org/0000-0002-2376-6979
M. Gu https://orcid.org/0000-0002-4267-9344
B. A. Joshi https://orcid.org/0000-0002-7593-8584
T. Li https://orcid.org/0009-0005-5008-0381
S. Schuldt https://orcid.org/0000-0003-2497-6334
L. G. Strolger https://orcid.org/0000-0002-7756-4440
S. H. Suyu https://orcid.org/0000-0001-5568-6052
G. B. Caminha https://orcid.org/0000-0001-6052-3274
S. H. Cohen https://orcid.org/0000-0003-3329-1337
J. M. Diego https://orcid.org/0000-0001-9065-3926
J. C. J. DSilva https://orcid.org/0000-0002-9816-1931
S. Ertl https://orcid.org/0000-0002-5085-2143
B. L. Frye https://orcid.org/0000-0003-1625-8009
G. Granata https://orcid.org/0000-0002-9512-3788
C. Grillo https://orcid.org/0000-0002-5926-7143
A. M. Koekemoer https://orcid.org/0000-0002-6610-2048
J. Li https://orcid.org/0000-0002-8184-5229
A. Robotham https://orcid.org/0000-0003-0429-3579
J. Summers https://orcid.org/0000-0002-7265-7920
T. Treu https://orcid.org/0000-0002-8460-0390
R. A. Windhorst https://orcid.org/0000-0001-8156-6281
A. Zitrin https://orcid.org/0000-0002-0350-4488
S. Agarwal https://orcid.org/0000-0002-2350-4610
A. Agrawal https://orcid.org/0009-0008-1965-9012
N. Arendse https://orcid.org/0000-0001-5409-6480
S. Belli https://orcid.org/0000-0002-5615-6018
C. Burns https://orcid.org/0000-0003-4625-6629
R. Cañameras https://orcid.org/0000-0002-2468-5169
S. Chakrabarti https://orcid.org/0000-0001-6711-8140
W. Chen https://orcid.org/0000-0003-1060-0723
T. E. Collett https://orcid.org/0000-0001-5564-3140
D. A. Coulter https://orcid.org/0000-0003-4263-2228
R. S. Ellis https://orcid.org/0000-0001-7782-7071
M. Engesser https://orcid.org/0000-0003-0209-674X
N. Foo https://orcid.org/0000-0002-7460-8460
O. D. Fox https://orcid.org/0000-0003-2238-1572
C. Gall https://orcid.org/0000-0002-8526-3963
N. Garuda https://orcid.org/0000-0003-3418-2482
S. Gezari https://orcid.org/0000-0003-3703-5154
S. Gomez https://orcid.org/0000-0001-6395-6702
K. Glazebrook https://orcid.org/0000-0002-3254-9044
J. Hjorth https://orcid.org/0000-0002-4571-2306
X. Huang https://orcid.org/0000-0001-8156-0330
S. W. Jha https://orcid.org/0000-0001-8738-6011
P. S. Kamieneski https://orcid.org/0000-0001-9394-6732
P. Kelly https://orcid.org/0000-0003-3142-997X
C. Larison https://orcid.org/0000-0003-2037-4619
L. A. Moustakas https://orcid.org/0000-0003-3030-2360
M. Pascale https://orcid.org/0000-0002-2282-8795
I. Pérez-Fournon https://orcid.org/0000-0002-2807-6459
T. Petrushevska https://orcid.org/0000-0003-4743-1679
F. Poidevin https://orcid.org/0000-0002-5391-5568
A. Rest https://orcid.org/0000-0002-4410-5387
M. Shahbandeh https://orcid.org/0000-0002-9301-5302
A. J. Shajib https://orcid.org/0000-0002-5558-888X
M. Siebert https://orcid.org/0000-0003-2445-3891
C. Storfer https://orcid.org/0000-0002-0385-0014
Q. Wang https://orcid.org/0000-0001-5233-6989
T. Wevers https://orcid.org/0000-0002-4043-9400
Y. Zenati https://orcid.org/0000-0002-0632-8897

References

Akhshik, M., Whitaker, K. E., Leja, J., et al. 2023, ApJ, 943, 179
Arendse, N., Dhawan, S., Sagués Carracedo, A., et al. 2023, arXiv:2312.04621
Birrer, S., Dhawan, S., & Shajib, A. J. 2022a, ApJ, 924, 2
Birrer, S., Millon, M., Sluse, D., et al. 2022b, arXiv:2210.10833
Birrer, S., Shajib, A. J., Galan, A., et al. 2020, A&A, 643, A165
Birrer, S., Treu, T., Rusu, C. E., et al. 2019, MNRAS, 484, 4726
Blondin, S., & Tonry, J. L. 2007, ApJ, 666, 1024
Bonvin, V., Chan, J. H. H., Millon, M., et al. 2018, A&A, 616, A183
Bonvin, V., Courbin, F., Suyu, S. H., et al. 2017, MNRAS, 465, 4914
Bonvin, V., Millon, M., Chan, J. H.-H., et al. 2019, A&A, 629, A97
Boyer, M. L., Anderson, J., Gennaro, M., et al. 2022, RNAAS, 6, 191
Burud, I., Hjorth, J., Courbin, F., et al. 2002, A&A, 391, 481
Bushouse, H., Eisenhamer, J., Dencheva, N., et al. 2022, JWST Calibration Pipeline, v1.12.5, Zenodo, doi:10.5281/zenodo.7325378
Chen, G. C. F., Fassnacht, C. D., Suyu, S. H., et al. 2019, MNRAS, 490, 1743
Chen, W., Kelly, P., Castellano, M., et al. 2022, TNSTR, 2022-3517, 1
Chen, W., Kelly, P. L., Frye, B. L., et al. 2024, arXiv:2403.19029
Craig, P., O'Connor, K., Chakrabarti, S., et al. 2021, arXiv:2111.01680
Dhawan, S., Johansson, J., Goobar, A., et al. 2020, MNRAS, 491, 2639
Ding, X., Liao, K., Birrer, S., et al. 2021, MNRAS, 504, 5621
Falco, E. E., Gorenstein, M. V., & Shapiro, I. I. 1985, ApJL, 289, L1
Foxley-Marrable, M., Collett, T. E., Vernardos, G., Goldstein, D. A., & Bacon, D. 2018, MNRAS, 478, 5081
Fremling, C., Miller, A. A., Sharma, Y., et al. 2020, ApJ, 895, 32
Freundlich, J., & Maoz, D. 2021, MNRAS, 502, 5882
Frye, B. L., Pascale, M., Pierel, J., et al. 2024, ApJ, 961, 171
Goldstein, D. A., Nugent, P. E., Kasen, D. N., & Collett, T. E. 2018, ApJ, 855, 22
Goobar, A., Amanullah, R., Kulkarni, S. R., et al. 2017, Sci, 356, 291
Goobar, A., Johansson, J., Schulze, S., et al. 2023, NatAs, 7, 1098
Grillo, C., Pagano, L., Rosati, P., & Suyu, S. H. 2024, A&A, 684, L23
Grillo, C., Rosati, P., Suyu, S. H., et al. 2018, ApJ, 860, 94
Grillo, C., Rosati, P., Suyu, S. H., et al. 2020, ApJ, 898, 87
Guy, J., Sullivan, M., Conley, A., et al. 2010, A&A, 523, A7
Hjorth, J., Burud, I., Jaunsen, A. O., et al. 2002, ApJL, 572, L11
Holz, D. E. 2001, ApJL, 556, L71
Hsiao, E. Y., Conley, A., Howell, D. A., et al. 2007, ApJ, 663, 1187
Huber, S., Suyu, S. H., Noebauer, U. M., et al. 2021, A&A, 646, A110
Ivezic, Z., Kahn, S. M., Tyson, J. A., et al. 2019, ApJ, 873, 111
Jones, D. O., Foley, R. J., Narayan, G., et al. 2021, ApJ, 908, 143
Kelly, P., Zitrin, A., Oguri, M., et al. 2022, TNSAN, 169, 1

Kelly, P. L., Rodney, S., Treu, T., et al. 2023a, Sci, 380, abh1322
Kelly, P. L., Rodney, S., Treu, T., et al. 2023b, ApJ, 948, 93
Kelly, P. L., Rodney, S. A., Treu, T., et al. 2015, Sci, 347, 1123
Kelly, P. L., Rodney, S. A., Treu, T., et al. 2016, ApJL, 819, L8
Kelsey, L. 2024, MNRAS, 527, 8015
Kenworthy, W. D., Jones, D. O., Dai, M., et al. 2021, ApJ, 923, 265
Koekemoer, A. M., Faber, S. M., Ferguson, H. C., et al. 2011, ApJ, 197, 36
Kolatt, T. S., & Bartelmann, M. 1998, MNRAS, 296, 763
Krisciunas, K., Contreras, C., Burns, C. R., et al. 2017, AJ, 154, 211
Kroupa, P. 2001, MNRAS, 322, 231
Kundić, T., Turner, E. L., Colley, W. N., et al. 1997, ApJ, 482, 75
Leget, P.-F., Gangler, E., Mondon, F., et al. 2020, A&A, 636, A46
Li, W., Chornock, R., Leaman, J., et al. 2011, MNRAS, 412, 1473
Linder, E. V. 2011, PhRvD, 84, 123529
Mandel, K. S., Thorp, S., Narayan, G., Friedman, A. S., & Avelino, A. 2022, MNRAS, 510, 3939
Maoz, D., Mannucci, F., & Brandt, T. D. 2012, MNRAS, 426, 3282
Narayan, R., & Bartelmann, M. 1997, arXiv:astro-ph/9606001
Newman, A. B., Belli, S., Ellis, R. S., & Patel, S. G. 2018, ApJ, 862, 125
Nordin, J., Rubin, D., Richard, J., et al. 2014, MNRAS, 440, 2742
Oguri, M. 2019, RPPh, 82, 126901
Oguri, M., & Kawano, Y. 2003, MNRAS, 338, L25
Paraficz, D., & Hjorth, J. 2009, A&A, 507, L49
Pascale, M., Frye, B. L., Pierel, J. D. R., et al. 2024, arXiv:2403.18902
Patel, B., McCully, C., Jha, S. W., et al. 2014, ApJ, 786, 9
Pierel, J. D. R., Arendse, N., Ertl, S., et al. 2023, ApJ, 948, 115
Pierel, J. D. R., Frye, B. L., Pascale, M., et al. 2024, ApJ, 967, 50
Pierel, J. D. R., Jones, D. O., Kenworthy, W. D., et al. 2022, ApJ, 939, 11
Pierel, J. D. R., & Rodney, S. 2019, ApJ, 876, 107
Pierel, J. D. R., Rodney, S., Vernardos, G., et al. 2021, ApJ, 908, 190
Refsdal, S. 1964, MNRAS, 128, 307
Riess, A. G., Yuan, W., Macri, L. M., et al. 2022, ApJL, 934, L7
Rodney, S. A., Brammer, G. B., Pierel, J. D. R., et al. 2021, NatAs, 5, 1118
Rodney, S. A., Patel, B., Scolnic, D., et al. 2015, ApJ, 811, 70
Rose, B. M., Baltay, C., Hounsell, R., et al. 2021, arXiv:2111.03081
Salpeter, E. E. 1955, ApJ, 121, 161
Saunders, C., Aldering, G., Antilogus, P., et al. 2018, ApJ, 869, 167
Schechter, P. L., Bailyn, C. D., Barr, R., et al. 1997, ApJL, 475, L85
Scolnic, D., Smith, M., Massiah, A., et al. 2020, ApJL, 896, L13
Scolnic, D. M., Jones, D. O., Rest, A., et al. 2018, ApJ, 859, 101
Shajib, A. J., Birrer, S., Treu, T., et al. 2020, MNRAS, 494, 6072
Shajib, A. J., Mozumdar, P., Chen, G. C. F., et al. 2023, A&A, 673, A9
Smith, M., Sullivan, M., Wiseman, P., et al. 2020, MNRAS, 494, 4426
Strolger, L.-G., Rodney, S. A., Pacifici, C., Narayan, G., & Graur, O. 2020, ApJ, 890, 140
Suyu, S. H., Goobar, A., Collett, T., More, A., & Vernardos, G. 2024, SSRv, 220, 13
Suyu, S. H., Marshall, P. J., Auger, M. W., et al. 2010, ApJ, 711, 201
Tewes, M., Courbin, F., Meylan, G., et al. 2013, A&A, 556, A22
Toft, S., Zabl, J., Richard, J., et al. 2017, Natur, 546, 510
Treu, T., & Marshall, P. J. 2016, A&ARv, 24, 11
Treu, T., Suyu, S. H., & Marshall, P. J. 2022, A&ARv, 30, 8
Vuissoz, C., Courbin, F., Sluse, D., et al. 2008, A&A, 488, 481
Windhorst, R. A., Cohen, S. H., Jansen, R. A., et al. 2023, AJ, 165, 13
Wong, K. C., Suyu, S. H., Chen, G. C. F., et al. 2020, MNRAS, 498, 1420
Xu, D., Sluse, D., Schneider, P., et al. 2016, MNRAS, 456, 739
Yahalomi, D. A., Schechter, P. L., & Wambsganss, J. 2017, arXiv:1711.07919